SCIENTIFIC PAPER

The Influence of Vibration Velocity on the Nano Composite of Halloysite Clay Nanotubes

Behrooz Sedighi[1], Abolfazl Davodiroknabadi[2*], Mohammad Shahvaziyan[1], Mohammadali Shirgholami[1]

[1]*Department of Textile Engineering, Yazd Branch, Islamic Azad University, Yazd, Iran*

[2]*Department of Design and Clothing, Yazd Branch, Islamic Azad University, Yazd, Iran*

https://doi.org/10.2298/CICEQ240712003S

Received 12.7.2024.

Revised 28.1.2025.

Accepted 6.2.2025.

* Corresponding Author Email: davodi@iauyazd.ac.ir , +983531872550

Abstract

This research examined the properties of a nano web created using the electrospinning technique, incorporating Halloysite clay nanotubes. The main focus was to understand how different vibration speed affected the characteristics of the nano web. By utilizing FESEM and elemental mapping, it was confirmed that the Halloysite clay nanotubes were present and provided valuable insights into the structure of the samples. The results regarding electrical conductivity were remarkable, showing that the treated specimens had higher crease recovery properties compared to the untreated ones(more than 24%), thanks to the presence of Halloysite clay nanotubes and the different vibration speed applied. In addition, the samples showed improved UV blocking capabilities up to about 75%, as well as exceptional strength (~33%) and resistance to abrasion (~93%). Overall, the nanocomposite webs exhibited promising qualities that could have applications in various industries.

Keywords: Clay Nanotubes, Vibration Speed, Electrospinning, Nano Web

Highlights

Influence of Vibration Velocity on Composite Properties.

Enhancing Electrical Conductivity of Composite.

Enhancing Crease Recovery of Composite.

Introduction

Nano web/fiber electrospinning is a cutting-edge technology that has the potential to revolutionize various industries, including healthcare and electronics. By harnessing the power of an electric field, electrospinning produces polymer webs that have a wide range of applications. These applications span across tissue engineering, drug delivery systems, filtration, and sensors. One particularly exciting application is in regenerative medicine, where these nano fibers can serve as scaffolds to support tissue regeneration. This process mimics the natural extracellular matrix and aids in the healing and restoration of damaged organs and tissues. Moreover, the small size of these webs facilitates cell adhesion and growth, which holds great promise for advancements in the treatment of injuries and diseases. Additionally, this technique can be utilized to create nano composites using natural materials [1-9].

In order to create a nanocomposite, Ghiasi et al. conducted a study that involved extracting active components from wheat bran using this particular method. According to their findings, the resulting composite contained nanomaterials and exhibited advantageous characteristics in terms of protection against ultraviolet rays and bacteria [10]. In contrast, Zohoori et al. conducted a study where they utilized palm-based materials and carbon mesoporous nanoparticles to create a nanocomposite through the electrospinning method. This investigation demonstrated the effectiveness of electrospinning in the production of nanocomposites and achieved positive outcomes in enhancing the properties of the nanocomposite [11]. Asakereh and his team conducted additional research by utilizing the technique of electrospinning to create nanocomposites using hazelnut green shells. Through their study, they successfully synthesized nanocomposites made of gelatin and hazelnut green shells, which exhibit unique properties [12]. Nano membranes and nano composites offer a broad spectrum of applications that enhance various attributes, including water-attracting capabilities, permeability to substances, salt rejection capacity, resistance to fouling, and long-lasting durability [13]. In recent times, there has been a significant increase in the focus on natural composites. This is because these composites possess unique characteristics such as effective sound insulation, recyclability, easy accessibility, and environmental friendliness. These properties are achieved by incorporating nanomaterials into the composites. Currently, a wide range of nanomaterials is being utilized to enhance specific qualities in the final products. One example of such a nanomaterial is nano clay. Nano clay is known for its impressive strength-to-weight ratio, meaning that despite being lightweight, it exhibits remarkable strength and durability. Additionally, nano clay possesses exceptional barrier capabilities. Its extremely

small size and unique structure enable it to form a tight network of particles, acting as a barrier against gases and liquids [14-21].

The study conducted by Gbadeyan et al. discovered that the addition of nano clay to banana fibers enhances the bonding between the matrix, nano clay, and banana fiber. This improvement is attributed to the thermal properties and hydrophobic nature of the nano clay, as well as the enhanced capacity of the banana fiber to distribute stress within the bio composites. As a result, there is a significant enhancement in the dynamic mechanical analysis, rate of water absorption, and abrasion properties [22]. Nano fibers and nano webs, despite their lack of electrical conductivity, possess certain limitations in terms of their properties. The occurrence of static electricity in nano webs leads to their adherence to the surrounding environment, causing discomfort when worn. Additionally, static electricity poses a disadvantageous factor in knitting and weaving processes, possibly resulting in fabric damage. Numerous approaches exist for investigating the electrical conductivity of these materials [23-27].

This study presents a novel approach to the creation of a nanocomposite by incorporating Halloysite clay nanotubes and subjecting the material to varying vibration speeds during its synthesis. The findings are groundbreaking, particularly in the realm of electrical conductivity, where the treated specimens outperformed their untreated counterparts. The incorporation of Halloysite clay nanotubes, coupled with the effects of controlled vibration speeds, significantly enhanced crease recovery properties, making the material more versatile for practical applications. Additionally, the nanocomposite demonstrated improved UV blocking capabilities and exceptional mechanical properties, including strength and resistance to abrasion. These advancements underscore the potential of this innovative methodology in developing high-performance materials for diverse industrial applications.

The primary objective of this study involved the creation of a nano composite by utilizing Halloysite clay nanotubes with the application of different vibration speed. The aim was to assess the diverse attributes of the composite and establish a versatile nano structure. Rather than depending on chemical particles, this research opted for the integration of nano particles and vibration energy as a doping agent to augment the characteristics of nano composites.

Experimental

Materials and Devices

Halloysite clay nanotube ($Al_2Si_2O_5(OH)_4 \cdot 2H_2O$) with surface area of 64 m^2/g and molecular weight of 294.19 was prepared from Sigma Aldrich (CAS No.1332-58-7). Tetra-ammine-di-aqua-copper(II) hydroxide with formula of $[Cu(NH_3)_4(H_2O)_2](OH)_2$ and succinic

acid (CAS No.110-15-6) as a cross-link factor was prepared from Merck. The strength under tension was analyzed using a tabletop uniaxial testing device called INSTRON 3345. To achieve homogeneity in the solution, a high energy micro-vibration homogenizer (model MSK-SFM-12M-LD) was utilized. The abrasion resistance was evaluated using the ASTM D-3884-09 method, employing a double-head rotary platform. We examined the morphology of the specimens by utilizing a field emission scanning electron microscope (FESEM-MIRA3-TESCAN). To enhance visibility, a thin layer of gold film was applied onto the samples. Magnetic stirrer (Model: HPMA 700) was used to prepare solution. In order to gauge the level of electrical conductivity, we utilized the Hioki digital multimeter model 3256/50 from Japan. Also, crease recovery tester device model GT-C21-1(China) was used. The crystalline structure of the materials was characterized by X-Ray Diffraction model Bruker D8 Discover, Germany.

Method

Pure cellulose was liquefied utilizing Schweizer's reagent, also identified as ($[Cu(NH_3)_4(H_2O)_2](OH)_2$). This liquefaction phase lasted for half an hour, conducted with a magnetic stirrer at 60°C. In the next step, succinic acid was infused into the concoction, accompanied by Halloysite clay nanotubes of 1.5% concentration. This newly formed compound was then agitated for another half-hour at the same temperature of 60°C, utilizing a magnetic stirrer. Following this, the concoction was subjected to a high-intensity micro-vibration homogenizer employing a device with vibration speeds of 2700, 3500, and 4000 rpm, at a temperature of 50°C for 3 minutes. The final blend was then divided into three different syringes situated on an electrospinning machine. The end result of this operation was the successful creation of a nonwoven web.

Table1.

Results and Discussion

Morphological Analysis

An in-depth exploration of the physical properties of nanofibers produced via electrospinning necessitates a meticulous study of their microscopic architecture. This examination enables us

to understand the layout, dispersal, dimensions, form, and surface attributes of these nanofibers. By employing state-of-the-art visualizing methods such as field emission scanning electron microscopy (FESEM), we can procure intricate, high-definition images that display the complex aspects of these fibers. This inclusive review offers precious knowledge on how elements like polymer density, electric charge, and solvent mix impact the construct of electrospun nanofibers. Figure 1 portrays a field emission scanning electron microscopy visual of the specimen, indicating that the cross-section of the nanocomposite is about 59nm. Moreover, Figure 1(A-B) demonstrates that the nanofibers are synthesized via electrospinning. Upon a more detailed scrutiny, it's evident that the breadth of the nanofibers doesn't surpass 75nm, which is exceptionally satisfactory. Upon scrutiny of the distribution of Halloysite clay nanotubes, it becomes evident that they approximately span 34nm Figure 1(C). Moreover, their configuration is distinctly portrayed through the visual depiction. The images we acquired suggest that the parameters set for electrospinning have been successful, considering there are no major signs of necking in the FESEM analysis conducted. On the other hand, a frozen section image is captured to confirm the internal presence of the nanotubes. For this purpose, a small portion of the web is collected and rapidly frozen using liquid nitrogen to maintain its structural integrity. Subsequently, a microtome designed for frozen samples is employed to slice the frozen sample into thin sections (Figure1(D)). This image reveals that the Halloysite clay nanotubes are moderately evenly distributed within the fibrous network, with minor clustering observed in select regions. The nanotubes retain their tubular structure and remain intact, with no significant deformation visible. There is clear evidence of close interaction between the cellulose fibers and the nanotubes, suggesting good integration within the composite structure. The fibers exhibit consistent diameters and smooth surfaces, indicative of uniform electrospinning conditions.

Figure1.

X-Ray Diffraction Analysis

Figure2 shows the XRD pattern of sample. The XRD pattern shows that the electrospinning process successfully integrates kaolin clay nanotubes and cellulose into a

composite material. Both components retain their distinct crystalline characteristics while forming a stable physical mixture. The chart indicates a high potential for the material's use in applications requiring a hybrid of strength, adsorption, and biodegradability. Here's a detailed analysis of the chart:

- Kaolin Clay Peaks:
  - A sharp peak at approximately **12° 2θ**, indicative of kaolinite's basal plane reflections.
  - A moderate peak at around **20° 2θ**, associated with higher-order reflections from kaolin.
  - A distinct peak near **25° 2θ**, commonly attributed to structural lattice planes of kaolinite.
  - A broad peak at **35° 2θ**, characteristic of less intense but significant kaolinite reflections.
  - A sharp peak at **62° 2θ**, a higher-angle reflection related to kaolinite's crystalline structure.
- Cellulose Peaks:
  - A smaller but noticeable peak at **15° 2θ**, corresponding to the amorphous phase of cellulose.
  - A strong and sharp peak at **22° 2θ**, the most prominent cellulose peak, associated with the crystalline plane (200) of cellulose I.
  - A weaker but evident peak at **34° 2θ**, related to less prominent crystalline planes in cellulose.

The XRD diagram reveals a composite structure where kaolin nanotubes and cellulose retain their distinct crystalline and amorphous characteristics, enabling synergistic interactions that enhance electrical conductivity. The sharp peaks of kaolin indicate its ordered nanotube structure, which acts as a scaffold for charge transfer, while the crystalline and amorphous regions of cellulose contribute mechanical flexibility and ionic mobility, respectively. The uniform dispersion of kaolin within the cellulose matrix, facilitated by the electrospinning process, minimizes resistance and creates interconnected pathways for electron and ion transport. This combination of structural order, physical interaction, and charge mobility results in a composite with improved electrical conductivity compared to its individual components.

The conductive network in the composite is formed despite the uneven distribution of clay nanotubes due to percolation theory, where sufficient connectivity among nanotubes enables electron or ion transport. The high aspect ratio of the nanotubes ensures overlapping conductive pathways, while the cellulose matrix supports ionic mobility in regions with fewer nanotubes. Localized zones of higher nanotube concentration compensate for less dense areas, allowing the composite to maintain conductivity.

The enhanced interface between the clay nanotubes and cellulose nanofibers arises from the electrospinning process, which embeds the nanotubes into the matrix and promotes strong interfacial adhesion through hydrogen bonding. The alignment of cellulose chains around the nanotubes during spinning and potential surface functionalization of the clay further improve compatibility and charge transfer. Together, these factors create a hybrid structure that balances conductivity with mechanical stability, even with non-uniform nanotube distribution.

The enhanced interface between Halloysite nanoclay (HNTs) and the electrospun cellulose matrix is primarily attributed to specific chemical and physical interactions that improve adhesion, dispersion stability, and charge transfer. One of the dominant mechanisms is “hydrogen bonding”, where hydroxyl (-OH) groups on both Halloysite and cellulose form strong intermolecular bonds, ensuring a stable interface and uniform dispersion. Additionally, “van der waals forces” contribute to stabilizing the nanotube dispersion within the matrix, preventing agglomeration. The electrospinning process further enhances interfacial interaction through “mechanical interlocking”, where the high shear forces align cellulose chains around the nanotubes, creating a physically integrated structure that improves stress transfer. If the nanotubes undergo “chemical functionalization”, such as Silane coupling or carboxylation, “covalent bonding” can be introduced, forming a more permanent attachment to the cellulose matrix, which further strengthens mechanical integrity and charge transfer. Moreover, “ionic interactions” may occur if functionalized nanotubes carry opposite charges to the cellulose, enhancing dispersion stability and conductivity. These interactions collectively improve the composite’s performance by reducing nanotube aggregation, increasing mechanical strength, and optimizing charge mobility.

Figure2.

Abrasion and Strength Properties

Throughout their existence, nanocomposites such as nano-webs experience a range of pressures and strains. Known for their minuscule size and remarkable resilience, nano-webs have instigated considerable transformations across various sectors. To assess the effects of wear and tear, a friction test involving 10 cycles was carried out to calculate the shift in the sample's mass pre and post-test. As depicted in Table 2, all processed samples show outstanding resistance against wear and tear. Even post 10 friction cycles, they uphold a resistance rate

above 91%. When we contrast samples A, B, C, and D, there's a marked disparity in their resistance to wear. Sample A, employed as a control specimen, showed zero resistance, while the remaining samples exhibited maximum resistance. This difference can be credited to the increased interfacial interactions within the webs, enabled by Halloysite clay nanotubes. These interactions result in superior load distribution and resistance to deformation. The large surface area and distinct surface chemistry of Halloysite clay nanotubes foster robust bonding with the nearby polymer matrix, contributing to this occurrence.

Sample C's remarkable sturdiness can be attributed to the inclusion of Halloysite clay nanotubes and a 3500 rpm vibrational treatment. Elevating the rpm results in enhanced resilience and strength. Nevertheless, surpassing 3500 rpm results in a minor decline in these characteristics. This happens due to excessive power causing an increase in heat, which could adversely affect the polymer solution or solvent involved in the electrospinning process.

To evaluate the durability of the samples, tension tests were performed on the produced nanofibers. The results showed that the treated specimens displayed impressive lastingness. This is a significant observation since the robustness of these nano-webs exceeds that of the control sample. The exceptional toughness of these webs is due to their unique molecular structure and makeup. Comprised of extended chains of organic molecules closely packed, the webs form a compact and sturdy material. This particular configuration allows the nano-webs to withstand considerable stress and strain without showing signs of cracks or distortions. Additionally, the nano webs display an exceptional ability to resist wear and tear, demonstrating their potential to endure degradation from friction.

Table2.

Crease Recovery Property

Crease recovery properties refer to the resilience of a rectangular fiber piece when it's subjected to a certain load and folded for a specific timeframe. This property measures the fiber's ability to bounce back to its original state without wrinkles. This is gauged by the angle created between the halves before it was folded, commonly known as the crease recovery angle. During this experiment, samples measuring 40*15mm were trimmed and evaluated to

determine crease recovery. The ultimate recorded value of the crease recovery angle represents an average of five separate measurements.

Table2 shows the influence of different finishing conditions on the crease recovery characteristic of the nano web at various vibration speeds. Clearly, the processed samples showed a substantial rise of more than 13% in the angle of crease recovery. In particular, sample C revealed the greatest enhancement, with an increase of around 19%, while sample D showcased a significant rise of nearly 18%. A key factor for this improved crease recovery in nanofibers that contain clay nanotubes is their unique formation. Clay nanotubes are known for their high aspect ratio and hollow tubular design, which grants them the ability to give mechanical support to the nanofibers. Having these clay nanotubes within the nanofiber matrix amplifies the total rigidity and structural soundness of the material, thereby boosting its capability to bounce back from creases. Moreover, clay nanotubes also have a high surface area enabling them to create robust interfacial bonds with the polymer matrix of the nanofibers. The robust bonding at the interface of the clay nanotubes and the polymer matrix aids in efficiently spreading and relieving mechanical strains, thus avoiding lasting distortion of the substance.

A detailed scrutiny of the results reveals a minor reduction in crease recovery as the vibration speed surpasses 3500 rpm. This phenomenon is likely caused by potential instabilities in the electrospinning device when operating at higher speeds. On the flip side, an overuse of power can lead to increased heat production, which might adversely affect the polymer solution or solvent used during the electrospinning procedure.

Electrical Conductivity Analysis

The electrical conductivity or resistance of nano webs is a crucial feature that is frequently taken into account. Incorporating Halloysite clay nanotubes into the final web leads to an enhancement in electrical conductivity. Thorough analysis and comparison were conducted on all samples. The inclusion of nano material at various vibration speed greatly improved their conductivity. The findings demonstrate that samples B, C, and D exhibited conductivities of 10^{-8}, 10^{-6}, and 10^{-7} Ω/square, respectively. To put it simply, increasing the vibration speed does not have a significant impact on the electrical conductivity.

The findings align with the percolation theory, a theoretical framework used to improve the electrical conductivity of composites that include Halloysite clay nanotubes. This theory elucidates the formation of conductive pathways within the composite material by examining the connectivity and arrangement of the conductive Halloysite clay nanotube particles .

The introduction of clay nanotubes into the nano web structure enhances its electrical conductivity properties. These cylindrical nanoparticles consist of layered structures that offer excellent electrical conduction pathways. When integrated into the nano web matrix, these clay nanotubes establish a conductive network throughout the material. This network facilitates the movement of electrons, resulting in heightened electrical conductivity.

According to this theory, the achievement of a certain quantity of conductive particles leads to the creation of a continuous network that enhances the electrical conductivity. By adjusting the amount and arrangement of particles made from Halloysite clay nanotubes in the composite material, we have the ability to regulate electrical conductivity in order to fulfill specific application requirements. By examining the variables influencing conductivity, scientists can customize the characteristics of nano webs to meet particular needs. Additionally, the analysis of electrical conductivity offers valuable insights into the fundamental behavior of these materials at the nanoscale level. In summary, the analysis of electrical conductivity in nano webs that contain clay nanotubes is an essential area of research. It grants us the ability to comprehend and manipulate the electrical properties of these materials for diverse applications.

UV-Transmission Property

The investigation examined how UV radiation is transmitted within the wavelength range of 200 to 400 nm. The graphs in Figure 3 depict the transmission of UV rays through the nano webs. The data clearly indicates that the raw samples allow for greater UV transmission compared to the other samples, suggesting a significant distinction. Samples B-D, which contained nanoparticles, showed a decrease in UV transmission when compared to the control sample, indicating that the nano composite possessed UV blocking properties. Conversely, the incorporation of nanoparticles into the nano web resulted in improved UV blocking capabilities compared to the raw sample. This improvement can be attributed to the combined UV absorption of Halloysite clay nanotubes, as well as their ability to scatter and reflect UV radiation, thus preventing it from penetrating the skin and causing harm.

The ability of Halloysite clay nanotube webs to block UV radiation can be explained by multiple factors. Firstly, the distinct structure of Halloysite clay nanotubes enables them to efficiently scatter and absorb UV rays. The cylindrical shape of the nanotubes offers a significant surface area for interaction with UV photons, thereby enhancing the likelihood of

absorption. Furthermore, the internal hollow space of the nanotubes serves as a pathway for UV radiation, facilitating effective absorption and scattering across the entire web.

Moreover, the UV-blocking properties of Halloysite clay are also attributed to its chemical composition. Halloysite clay primarily consists of alumina and silica, both of which have demonstrated the ability to absorb UV radiation. Particularly, alumina possesses a high refractive index, enabling it to scatter and reflect UV rays. This scattering and reflection mechanism effectively prevents UV radiation from reaching the skin or any underlying materials beneath the nanotube webs. Additionally, the porous structure of Halloysite clay nanotube webs contributes to their UV-blocking capability. The presence of pores within the nanotube structure enhances light scattering and absorption, creating multiple interfaces for interaction with UV radiation. As a result, the likelihood of UV rays being absorbed or reflected before they can pass through the web is significantly increased.

The ability of Halloysite clay nanotube webs to block UV radiation is primarily due to their distinct structure, chemical composition, and porous characteristics. These attributes enable effective dispersion, reflection, and absorption of UV rays, safeguarding against their detrimental impacts. As a result, Halloysite clay nanotube webs hold great potential for use in products like sunscreens, protective clothing, and coatings for surfaces in need of UV protection.

Figure3.

Conclusion

The findings presented in this study suggest that varying the speed of vibration has an impact on the characteristics of the final nano webs product. Moreover, combining the method of composite fabrication with the use of Halloysite clay nanotubes can improve both the chemical and physical properties. The presence of Halloysite clay nanotube ions in the crystal lattice leads to an increase in the electrical-conductivity of the produced samples. These ions have the ability to move easily within the lattice, facilitating the flow of electric current. Doping Halloysite clay nanotubes also enhances the crease recovery ability of the samples up to 24%, although there is a slight decrease in crease recovery when the vibration speed exceeds 3500rpm. This decrease may be attributed to potential instabilities in the electrospinning

apparatus at higher speeds. Additionally, the nanocomposite exhibits superior UV-blocking capability compared to the raw samples due to its larger surface area-to-volume ratio (about 75%). Furthermore, the generated samples exhibited enhanced durability and resistance to wear, especially under the influence of a vibration speed reaching 3500rpm. This research not only provides valuable knowledge and understanding to the textile production industry but also deepens our comprehension of how various treatments can fundamentally modify the properties of nonwoven composites. Future research could explore the integration of Halloysite clay nanotubes with other functional additives to enhance multi-functional properties, such as thermal insulation or flame resistance, in textiles and composites. Additionally, optimizing vibration speeds and treatment methods could lead to tailored applications in smart fabrics, UV-protective clothing, and high-performance composite materials for aerospace or automotive industries.

Acknowledgment

This work was supported by Islamic Azad University-Yazd Branch.

Research ethics

Not applicable

Author contributions

BS designed this study, AD supervised the experimental work, MS revised the manuscript and MS worked in lab. The author read and approved the final manuscript.

Availability of data

Data available on request from the authors.

Conflict of Interest

All authors declare that they have no conflicts of interest.

Funding

This work was supported by Islamic Azad University-Yazd Branch (Award No.: 1403-01).

References

1. M. Mirjalili, S. Zohoori, J. Nanostruct. Chem. 6 (2016) 207. https://doi.org/10.1007/s40097-016-0189-y

2. S. Zohoori, M. Latifi, A. Davodiroknabadi, M. Mirjalili, Pol. J. Chem. Technol. 19 (2017) 56. https://doi.org/10.1515/pjct-2017-0049

3. A.S. Lebedev, A.V. Suzdal'tsev, V.N. Anfilogov, A.S. Farlenkov, N.M. Porotnikova, E.G. Vovkotrub, L.A. Akashev, Inorg. Mater. 56 (2020) 20. https://doi.org/10.1134/s0020168520010094

4. Y.V. Suvorova, S.I. Alekseeva, M.A. Fronya, I.V. Viktorova, Inorg. Mater. 49 (2013) 1357. https://doi.org/10.1134/s0020168513150089

5. A. Al-Attabi, M.A. Abdulhadi, L.R. Al-Ameer, M.D.N. Hussein, S.J. Abdulameer, R.S. Zabibah, A. Fadhil, Int. J. Mater. Res. 115 (2024) 162. https://doi.org/10.1515/ijmr-2023-0125

6. A. Davodiroknabadi, S. Zohoori, R. Talebikatieklahijany, F. Mohammadisaghand, S. Shahsavari, R. Mohammadisaghand, P. Zangeneh, Appl. Biochem. Biotechnol. (2024). https://doi.org/10.1007/s12010-024-04967-7

7. G. Esenoğlu, M. Barisik, M. Tanoğlu, M. Yeke, C. Türkdoğan, H. İplikçi, S. Martin, K. Nuhoğlu, E. Aktaş, S. Dehneliler, M.E. İriş, J. Compos. Mater. 56 (2022) 4449. https://doi.org/10.1177/00219983221133478

8. N. Sultana, R. Rahman, Emergent Mater. 5 (2022) 145. https://doi.org/10.1007/s42247-021-00326-y

9. D. Regmi, J. Choi, J. Xu, ECS Adv. 3 (2024) 4101. https://doi.org/10.1149/2754-2734/ad86cc

10. Y. Ghiasi, A. Davodiroknabadi, S. Zohoori, Bull. Mater. Sci. 44 (2021) 89. https://doi.org/10.1007/s12034-021-02406-5

11. S. Zohoori, S. Shahsavari, M. Sabzali, S. A. Hosseini, R. Talebikatieklahijany, Z. Morshedzadeh, J. Nat. Fibers. 19 (2022) 8937. https://doi.org/10.1080/15440478.2021.1975600

12. M. Asakereh, S. Zohoori, F. Mohammadisaghand, M. Sabzali, R. Mohammadisaghand, B. Soltani, J. Nat. Fibers. 19 (2022) 15552. https://doi.org/10.1080/15440478.2022.2131024

13. M. Alghamdi, A. El-Zahhar, Chem. Ind. Chem. Eng. Q. 27 (2021) 35. https://doi.org/10.2298/ciceq200128022a

14. R. Subramaniam, A. Eswaran, G. Sivasubramanian, A. Gurusamy, Emergent Mater. 6 (2023) 261. https://doi.org/10.1007/s42247-022-00434-3

15. S.M.U. Krithika, K. Mani, S.K. Thangavelu, C.M. Bharathi, K. Saravanan, C. Prakash, AATCC J. Res. 9 (2022) 213. https://doi.org/10.1177/24723444221103675

16. E.G. Il’in, A.S. Parshakov, S.Y. Kottsov, M.I. Razumov, D.Y. Gryzlov, Inorg. Mater. 58 (2022) 1130. https://doi.org/10.1134/s002016852211005x

17. V. Şimşek, M.O. Çağlayan, Int. J. Mater. Res. 114 (2023) 1047. https://doi.org/doi:10.1515/ijmr-2022-0491

18. A. Momeni, A. Ghadi, R. Fazaeli, M. Khavarpour, Int. J. Mater. Res. 114 (2023) 753. https://doi.org/doi:10.1515/ijmr-2021-8516

19. H. Salimimofrad, A. Rahbarranji, H. Saghafi, J. Compos. Mater. 58 (2024) 441. https://doi.org/10.1177/00219983231226277

20. N. Gupta, R. Maharsia, Appl. Compos. Mater. 12 (2005) 247. https://doi.org/10.1007/s10443-005-1130-6

21. S. Zohoori, N. Torabi, E. Gholami, F. Rastgoo, M. Rad, R. Pourheidari, Discover Mater. 4 (2024) 92. https://doi.org/10.1007/s43939-024-00164-9

22. O. Josephgbadeyan, T.P. Mohan, K. Kanny, Mater. Today: Proc. 87 (2023) 252. https://doi.org/10.1016/j.matpr.2023.05.352

23. S. Zohoori, M. Dolatshahi, M. Pourahmadi, M. Hajisafari, Fiber Integr. Opt. 38 (2019) 1. https://doi.org/10.1080/01468030.2019.1567871

24. R. Soltanisarvestani, S. Zohoori, A. Soltanisarvestani, Int. J. Electron. 107 (2020) 444. https://doi.org/10.1080/00207217.2019.1661027

25. S. Shamchi, X. Yi, P.M.G.P. Moreira, Appl. Compos. Mater. 30 (2023) 1. https://doi.org/10.1007/s10443-022-10070-z

26. N. Rac-Rumijowska, H. Teterycz, Mater. 16 (2023) 3085. https://doi.org/10.3390/ma16083085

27. A. Chanda, S. K. Sinha, N. Datla, Composites, Part A. 149 (2021) 106543. https://doi.org/10.1016/j.compositesa.2021.106543

Figure Captions

Figure1. FESEM of: (A,B) Electrospun sample, (C) Elemental map, (D) Frozen section

Figure2. XRD pattern of sample

Figure3. UV transmission diagram

Table1. Specification of samples

Sample	vibration speed (rpm)	Halloysite clay nanotube (%)
A	-	0.0
B	2700	1.5
C	3500	1.5
D	4000	1.5

Table2. Abrasion resistance, tensile strength and crease recovery angle of samples

Sample	Web weight before abrasion (g)	Web weight after abrasion (g)	Abrasion resistance (%)	Tensile strength(MPa)	Crease recovery angle(deg)
A	3.186	1.707	53.57	0.865	144
B	3.466	3.158	91.11	1.903	167
C	3.599	3.374	93.74	2.751	179
D	3.605	3.369	93.45	2.699	177

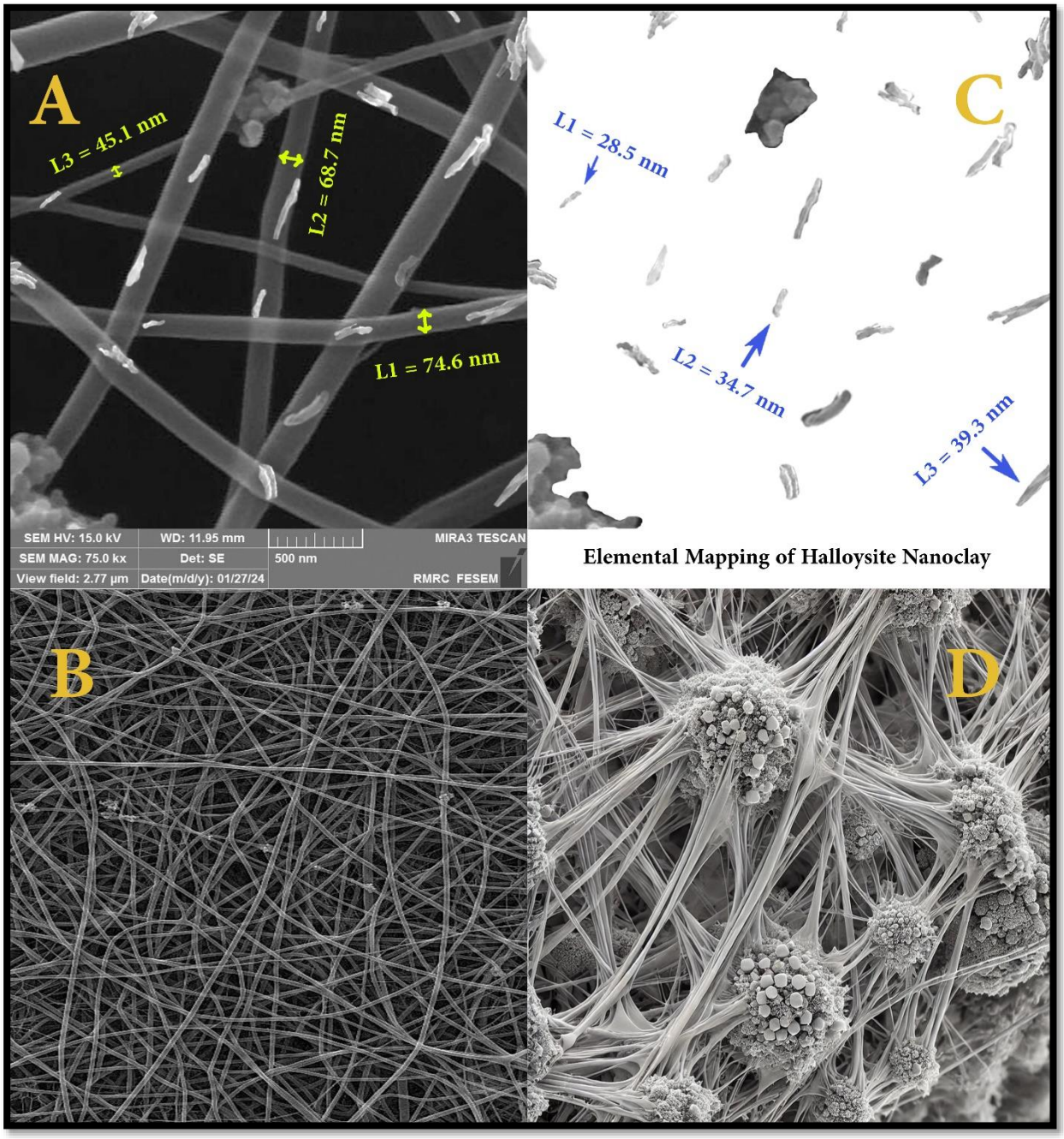
A
L3 = 45.1 nm
L2 = 68.7 nm
L1 = 74.6 nm
SEM HV: 15.0 kV
WD: 11.95 mm
MIRA3 TESCAN
SEM MAG: 75.0 kx
Det: SE
500 nm
View field: 2.77 µm
Date(m/d/y): 01/27/24
RMRC FESEM
C
L1 = 28.5 nm
L2 = 34.7 nm
L3 = 39.3 nm
Elemental Mapping of Halloysite Nanoclay
B
D

Figure 1

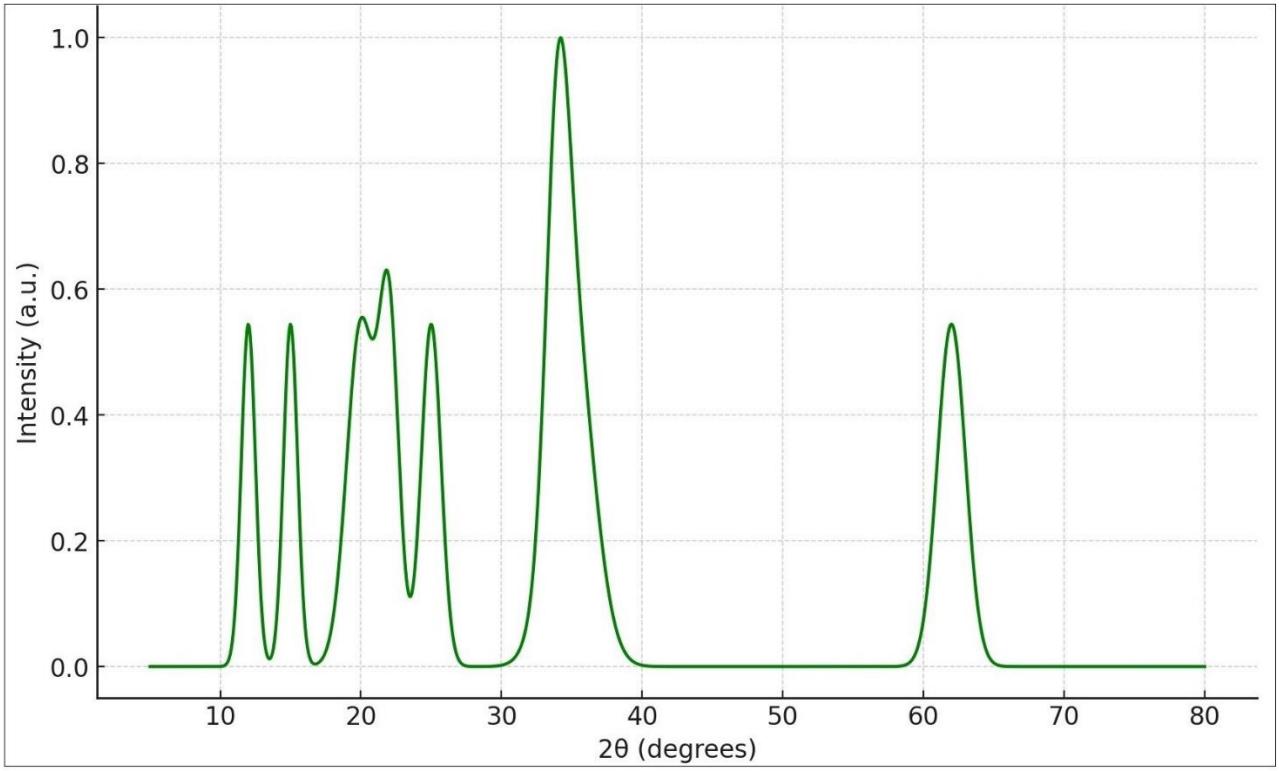

Figure 2

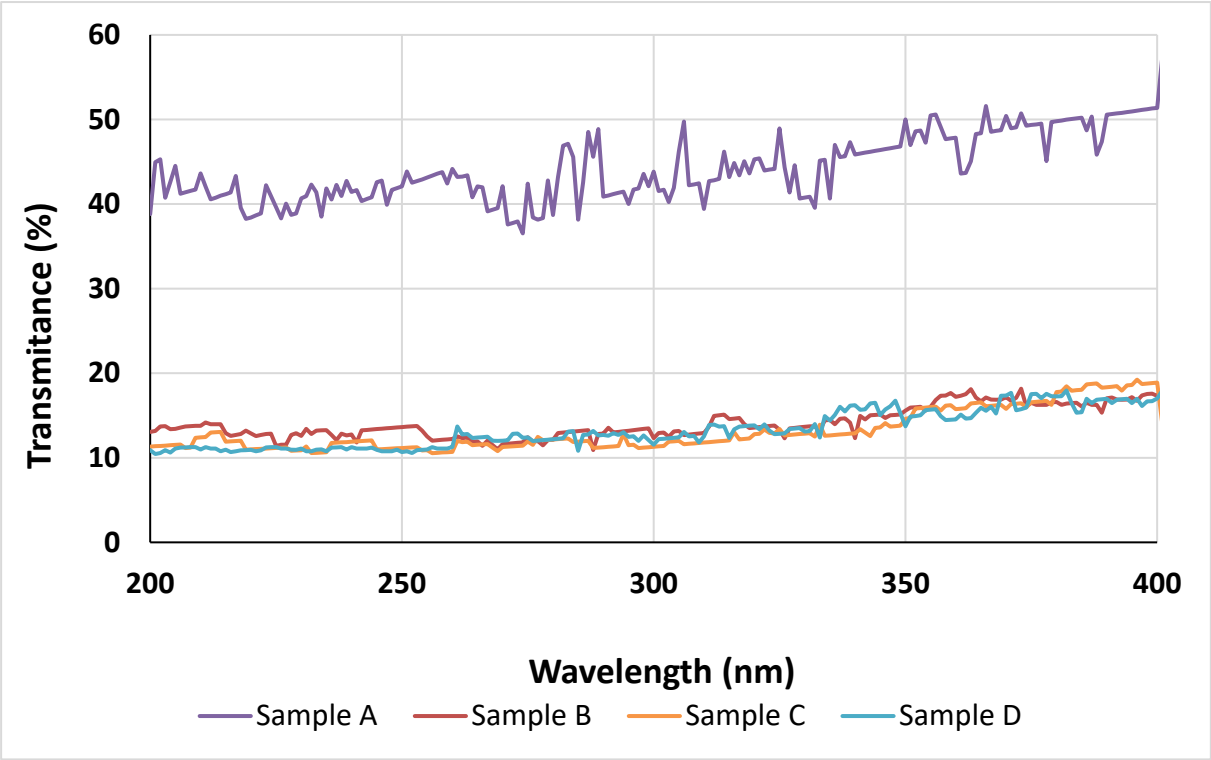
60
50
40
30
20
10
0
Transmitance (%)
200
250
300
350
400
Wavelength (nm)
Sample A
Sample B
Sample C
Sample D

Figure 3